VOL.39 Nº4 2022
https://doi.org/1022135\IMECTA.9896.en

Evaluation of the main open coaxial probe admittance models for electrical permittivity measurements

Daniel Henrique da Silva Souza[a], **José Carlos Araujo dos Santos**[b]

Engenharia Elétrica e Eletrônica - IME
[a]danhen.br@gmail.com
[b]araujo@ime.eb.br

RESUMO: O conhecimento preciso das propriedades dielétricas dos materiais, sobretudo permissividade, é essencial em diversas áreas da engenharia. O presente trabalho trata do método reflexivo de caracterização dielétrica baseado em sensores coaxiais. Apresenta uma avaliação criteriosa dos diversos modelos de admitância disponíveis na literatura para o sensor e uma comparação entre eles, de forma a evidenciar um modelo preciso e de computação rápida para implementação prática. Neste contexto, são abordados os dois problemas inerentes ao método da sonda coaxial, um relativo à determinação da admitância em função da permissividade (problema direto) e outro relativo à determinação da permissividade em função da admitância (problema inverso). No presente trabalho são consideradas as soluções do problema direto para os modelos da literatura.

PALAVRAS-CHAVE: Ponta de teste coaxial, sensor coaxial, coeficiente de reflexão, medidas de permissividade.

ABSTRACT: The accurate knowledge of the dielectric properties of materials, especially permittivity, is essential in several areas of engineering. The present work deals with the reflective method of dielectric characterization based on coaxial sensors. It presents an evaluation of various admittance models available in the literature for the sensor and a comparison between them, attempting to identify a fast and accurate model for practical applications. In this context, the two inherent problems to the coaxial probe method are addressed, one related to the admittance determination as a function of permittivity (direct problem) and another related to the permittivity determination as a function of admittance (reverse problem). In the present work, the solutions of the direct problem available in the literature are addressed.

KEYWORDS: Coaxial probe, open-ended coaxial sensor, reflection coefficient, permittivity measurement.

1. Introduction

The open-ended coaxial probe is a device widely used in the scientific-technological community for measuring the permittivity of liquids, solids and semi-solids within an extensive range of frequencies. In this context, associated coaxial probe, there are several measurement methods in the literature, which differ in complexity, reliability and precision.

EIn theory, a method for dielectric measurement with the coaxial probe should be able to determine the admittance of a material under test (MUT, from the English. *Material Under Test)* from a known value of permittivity. Thus, the so-called probe admittance models are established.

On the bench, the essence of the method consists of measuring the input reflection coefficient of the test probe immersed or in contact with the MUT and performing calculations, through suitable models, for extracting the permittivity, usually with the aid of CAD tools.

When there is an impedance difference between the transmission line of the coaxial probe and the material under evaluation at its open terminal, part of the incident signal on the sensor is absorbed by the material and part is reflected to the line. Functionally, the coaxial probe (or test lead) is a transmission line with an open end.

The basic structure of the probe is illustrated in **figure** 1, where a is the radius of the inner conductor, b is the radius of the outer conductorεc and is the low-loss dielectric that fills the transmission line of the probe. The open terminal, in the z = 0 plane, is formed by a flat metal flange that theoretically extends to infinity in the transverse direction.

The material to be measured is assumed to be homogeneous, isotropic, linear and non-magnetic, of permittivity complex relative, which must completely fill the half-spacez > 0.

The dimensions of the coaxial test lead and its upper operating frequency are selected to allow propagation of only the dominant TEM mode, which must be used to excite the lead and make measurements. The discontinuity that appears in the opening at z = 0 produces a reflection of the TEM wave, which propagates back to the coaxial line. Such a discontinuity also causes the appearance of higher order modes in the probe, evanescent, which, therefore, decay rapidly in the direction of the signal source. In the material, electromagnetic fields are radiated due to the TEM mode and higher modes (TM_{0n}) from the opening plan [1]. Only some admittance models consider higher order modes in the material. An important step in the complete characterization of a probe is to obtain a model that represents its real behavior.

Fig. 1 - Cross section of a coaxial test lead with indication of its dimensional parameters.

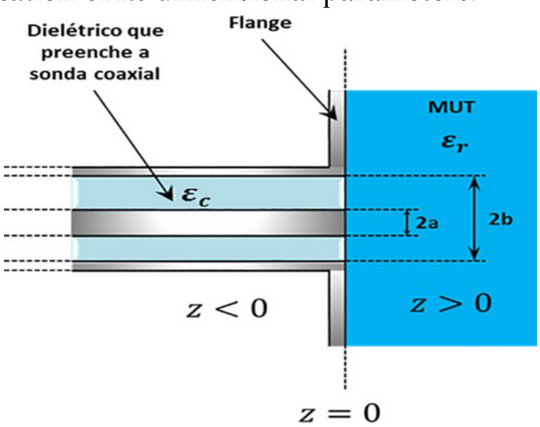

The coaxial probe method is, effectively, a "reflective method", in which the measurements are obtained from the reflection of an incident electromagnetic signal on the material[1].

Fig. 2 – Synthesis of the reflective method of measurement

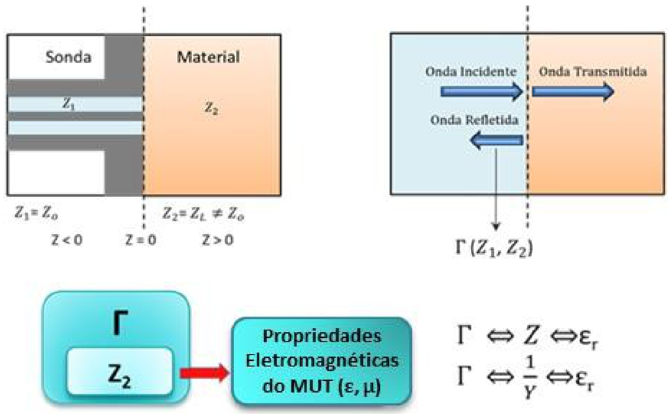

The essence of the method is represented in the **figure** 2. The termination open end of the probe is immersed in the medium under investigation or is put in contact with him. The reflection coefficient complex of this ending is uniquely related to the test signal frequency, probe parameters and permissiveness complex ε_r of material in test. For to determine εr precisely, It is necessary solve two problems:

a) The direct problem, where the admittance of the probe is determined as a function of permittivity.

$$Y = f(\varepsilon r) \tag{1}$$

b) The inverse problem, where permittivity is determined as a function of measured admittance.

$$\varepsilon_r = f{-}1(Y) \tag{2}$$

In both situations, the calculations are referenced to the opening plane of the probe (z = 0, in **figure** 3).

Both problems must be solved. The solution of the direct problem gives the material's real complex admittance (Y_{real}) or, equivalently, the material's real reflection coefficient (Γ_{real}), as (3). This value is required in calibration procedures with

https://doi.org/1022135\IMECTA.9896.en

the model of a network analyzer port.

$$Y_{real} = \frac{1 - \Gamma_{real}}{(1 + \Gamma_{real})} * YO \tag{3}$$

The solution of the inverse problem, on the other hand, provides the complex permittivity (ε_r), a qual é, de fato, o parâmetro que se deseja extrair do material.

which is, in fact, the parameter one wants to extract from the material.

Regarding the object of the present work, an extensive and varied range of admittance models can be found in the literature. Models based on the approximation of the probe to a concentrated equivalent circuit allow rapid determination of the complex permittivity [2] - [5]. In models based on the complete wave solution, rigorous electromagnetic analyses are performed in the half-spaces z < 0, z = 0 and z > 0, which involve techniques are usually computationally heavy [11] - [15].

There are models based on the simplification of the complete wave model that consider only the dominant mode HAS or that initially use only the mode HAS and then account for the higher order modes generated in the opening of the probe, from the adjustment of the theoretical model to experimental data [9], [18].

Finally, two other models stand out, one with the calculation of the complete wave from the method of moments and the adjustment of the result in a rational function to obtain the admittance equation [16], and the other based on an approximation of the relationship between reflection coefficient and permittivity to implement a bilinear function that relates the reflection coefficient and permittivity [16]. The solution of the inverse problem, on the other hand, provides the complex permittivity (ε_r), which is, in fact, the parameter one wants to extract from the material. Depending on the admittance model for the test tip, specific permittivity extraction techniques should be used.

This work is divided into five sections, including the current, introductory one. **section** 2 presents the main admittance models for the coaxial probe. **section** 3 summarizes the main permissiveness extraction techniques, according to the authors. **section** 4 presents a comparison between the models, deepening the analysis of the main characteristics of each one. **section** 5 presents the conclusions of the work.

2. Admittance Models For Coaxial Probe

An important step in the characterization of the probe is to obtain a forward model that approximates its actual behavior as much as possible.

The models proposed in the literature range from a simple equivalent circuit to those based on the numerical solution of Maxwell's equations and artificial intelligence techniques.

The present work provides an overview of the main existing models.

2.1 Capacitive model

In the capacitive model, the discontinuity in the termination of the coaxial probe is approximated by a concentrated equivalent circuit [2]. More precisely, the interface between the coaxial probe and the sample is modeled by two capacitors in parallel, as in **figure** 3, whose capacitances are considered to come from the probe 's internal dielectric edge fields (C_f) and from the sample's edge fields (C_o).

Fig. 3 – Discontinuity in the aperture modeled by two capacitances in parallel.

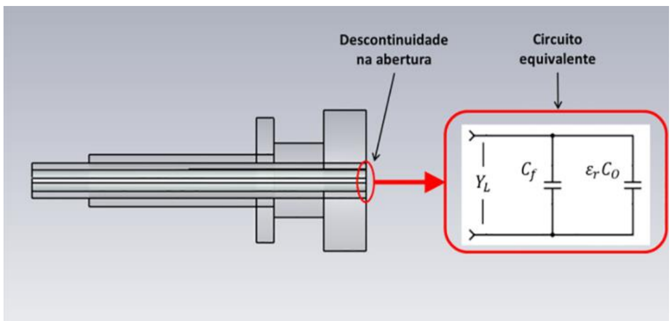

The discontinuity in the sensor aperture is then modeled as an admittance that relates to the capacitances Cf and Co through.

$$Y_L = j\omega Z_0 C_f + j\omega Z_0(\varepsilon' - j\varepsilon'')C_0 \tag{4}$$

where ω ω is the angular frequency, Z0 is the impedance of the coaxial cable (usually equal to 50Ω) and $(\varepsilon' - j\varepsilon'')C_0 = \varepsilon_r C_0 = C(\varepsilon_r)$.

The input reflection coefficient in the plane of discontinuity is then given by

$$\Gamma = |\Gamma| ej\phi \quad \frac{1 - j\omega Z0(\,C(\varepsilon r) + Cf)}{1 + j\omega Z0(\,C(\varepsilon r) + Cf)} \tag{5}$$

To obtain the capacitances of the capacitive model it is necessary to have two measures of reflection coefficient as a function of frequency, of two materials whose permittivity ε_r well known. These measurements of $\Gamma(f)$ are usually made with the network analyzer.

2.2 Radiation Models
2.2.1 Stuchly et al. Model

Stuchly et al. [4] [5] consider the coaxial probe as an irradiating source. Its model is an equivalent circuit of two capacitors (C_f, $\varepsilon_r C_0$), as in the capacitive model, and a conductance (G), connected in parallel, as in the **figure** 4. The Capacitance C_f concentration of electric field within the part of the coaxial line filled with the internal dielectric (teflon). The capacitance $\varepsilon_r C_0$ represents the edge electric field concentration in the external dielectric (of the MUT). The conductance G is the radiation conductance and relates to the power radiated from the termination of the coaxial probe.

Fig. 4 – Equivalent circuit for the radiation model [5].

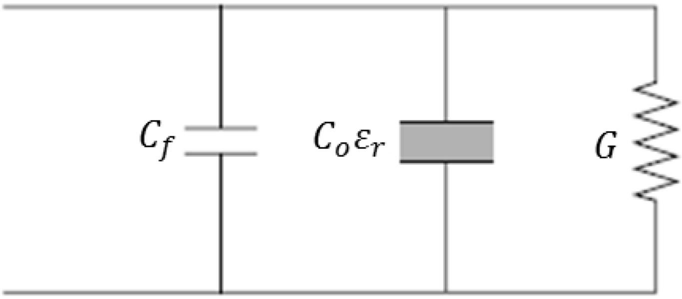

In this model, the normalized admittance is given by

$$\bar{Y} = \frac{Y}{Y_0} = j\omega C_f Z_0 + j\omega \varepsilon_r C_0 + \; Z_0 G(\,\omega, \varepsilon_r) \tag{6}$$

where Y_0 is the characteristic admittance of the line ($Z_0 = 1/Y_0$). For conductance, corresponding to an infinitesimal antenna, one writes [8].

$$G(\,\omega, \varepsilon_r) = \varepsilon_r{}^{5/2} G(\,\omega, \varepsilon_r) \tag{7}$$

2.2.2 Gadja and Stuchly model

Gadja and Stuchly [6] presented a more accurate model, given by

$$\frac{Y}{Y_0} = K_1 + K_2\varepsilon_r + K_3\varepsilon_r{}^2 + K_4\varepsilon_r{}^{5/2} \tag{8}$$

where the factors K_1, K_2, K_3 and K_4 are complex, calculated in the probe calibration process. Complex admittance is referenced to the termination plane of coaxial geometry.

2.2.3 Staebell and Misra model

Using quasi-static analysis, Staebell and Misra [7] provided the approximation

$$\frac{Y}{Y_0} = \mathrm{K}_1\,\varepsilon_r + K_2\varepsilon_r{}^2 + K_3\varepsilon_r{}^{5/2} \tag{9}$$

At low frequencies, this model becomes

$$\frac{Y}{Y_0} = K_1\varepsilon_r + K_2\varepsilon_r^{\,2} \qquad (10)$$

As in the previous model, the determination of the parameters K_i is achieved with calibration, and the permittivity is calculated from

$$\varepsilon = A - \frac{G_0}{\omega C_0}\, b \qquad (11)$$

$$\varepsilon = B - \frac{G_0}{\omega C_0}\, g \qquad (12)$$

where A and B are respectively the real and imaginary parts of the permittivity, calculated disregarding the radiation conductance, and b and g are dependent variables on the loss tangent and the real part of the permittivity [4] [5].

2.3 Quasi-static model

Marcuviz [4] presents an approximate formulation for a semi-infinite coaxial line terminated in an infinite metallic plane, radiating into free space (in the fundamental mode of the line). In its model, the admittance of the probe is expressed as an integral over its aperture, given by

$$Y_L = j\frac{k^2}{\pi k_c \ln(b/a)} \int_a^b \int_a^b \int_0^\pi \cos\phi' \frac{\exp(-jkr)}{r}\, d\varphi' d\rho' d\rho \qquad (13)$$

Fig. 5 – Geometry of the opening plane of the probe [9].

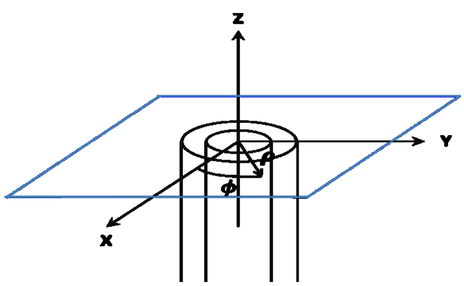

Misra [9] found that if the coaxial aperture is electrically very small, **equation** 13 can be approximated by the first two terms of its expansion in power series. This form corresponds to a quasi-static approximation to the Marcuvitz equation, being given by

$$\bar{Y}_L = \frac{Y}{Y_0} = j\frac{k^2}{\pi k_c \ln(b/a)} \int_a^b \int_a^b \int_0^\pi \left\{ \frac{\cos\phi'}{r} - jk\cos\phi' - \frac{k^2 r}{2}\cos\phi' + j\frac{k^3 r^2}{6}\cos\phi' \right\} d\phi' d\rho' d\rho \qquad (14)$$

Where;

$$Y_0 = \frac{2\pi}{\sqrt{\frac{\mu_0}{\varepsilon_0 \varepsilon_c}}\, ln\,(^b/_a)} \qquad (15)$$

Using the relation to the characteristic impedance of the coaxial line given by **equation** 15, the expression for the admittance at the probe aperture may be written as

$$Y_L = j\frac{2\omega\varepsilon_r}{[\ln(b/a)]^2}\left[I_1 - \frac{k^2 I_3}{2}\right] + \frac{k^3 \pi\omega\varepsilon_r}{12}\left[\frac{b^2 - a^2}{\ln(b/a)}\right]^2 \qquad (16)$$

Where;

$$I_1 = \int_a^b \int_a^b \int_0^\pi \frac{\cos\phi'}{[\rho^2 + \rho'^2 - 2\rho\rho'\cos\phi']^{1/2}} d\phi' d\rho' d\rho \qquad (17)$$

$$I_3 = \int_a^b \int_a^b \int_0^\pi \cos\phi' [\rho^2 + \rho'^2 - 2\rho\rho'\cos\phi']^{1/2} d\phi' d\rho' d\rho \qquad (18)$$

Quasi-static models represent an approximation that does not account for the excitation of higher-order modes in the aperture [12].

2.4 Expanded Marcuvitz model

In the so-called expanded Marcuvitz model, Misra [10] used Marcuvitz's original admittance expression and turned it into a series expansion of truncated power in 7 terms.

The results obtained showed that the model obtained is more accurate than the quasi-static model.

$$Y = G + jB \tag{19}$$

$$G = \frac{Y_{0\sqrt{\varepsilon_r}}}{\ln\left(b/a\right)\sqrt{\varepsilon_c}} \int_0^{\pi/2} \frac{1}{\sin\theta}\left[J_0\left(k_0\sqrt{\varepsilon_r}b\sin\theta\right) - J_0\left(k_0\sqrt{\varepsilon_r}a\sin\theta\right)\right]^2 d\theta \tag{20}$$

$$B = \frac{Y_{0\sqrt{\varepsilon_r}}}{\ln\left(b/a\right)\sqrt{\varepsilon_c}}$$

$$\int_0^{\pi}\left[2sen\left(k_0\sqrt{\varepsilon_r(a^2 + b^2 - 2abcos\theta)}\right) - sen\left(2k_0\sqrt{\varepsilon_r}a\sin(\theta/2)\right) - sen\left(2k_0\sqrt{\varepsilon_r}b\sin(\theta/2)\right)\right]d\theta \tag{21}$$

The main equations of expansion are:

$$B(f) = B^1(f) + B^2(f) + B^3(f) + B^4(f) + B^5(f) + B^6(f) + B^7(f) \tag{22}$$

$$G(f) = \frac{\sqrt{\frac{\varepsilon_r(f)}{\varepsilon_c}}}{ln\left[\frac{a}{b}\right]Zo}\left(G1(f) + G2(f) + G3(f) + G0(f) + G4(f) + G5(f)\right) \tag{23}$$

$$K1(f) = \frac{1}{Z_0\pi ln\left[\frac{a}{b}\right]}\sqrt{\frac{\varepsilon_r(f)}{\varepsilon_c}} \tag{24}$$

$$k(f) = \frac{2\pi f}{c}\sqrt{\varepsilon_r(f)} \tag{25}$$

Where $k(f)$ and $K^1(f)$ are complex functions of the permittivity of the material. $k(f)$ is the free space propagation constant and $K^1(f)$ is the propagation constant in the inner dielectric of the coaxial probe.

$B(f)$ and $G(f)$ are the susceptance and conductance of the material, that is, **equations** 20 and 21 expanded to a series of 7 and 5 terms, respectively. The other equations of the expansion are detailed in [10].

2.5 Full Wave Models

In the complete wave model, the electric and magnetic fields are evaluated in the regions $\mathbf{z < 0}$, $\mathbf{z = 0}$ **e** $\mathbf{z > 0}$. In this model a rigorous electromagnetic evaluation of the problem is carried out (irradiation of the open termination coaxial line, even to the free space, has no precise analytical solution). There are different variations to the full wave model [11] [15]. Most solutions involve variational techniques, which are computationally costly when looking for the solution to the inverse problem.

2.5.1 Levine and Popes Model

Levine and Papas [11] modeled an open-ended coaxial guide to free space with an equivalent circuit. The fundamental mode of propagation in the coaxial region has been theoretically investigated. The authors derived variational expressions for the circuit parameters and used **equation** 26 to obtain an accurate numerical evaluation of the coaxial line.

$$\frac{Y(0)}{Y_0} = \frac{G(0)}{Y_0} - \mathrm{i}\frac{B(0)}{Y_0} =$$

$$\frac{-ik}{\ln(b/a)}\int_0^{\infty}\frac{d_{\varsigma}}{\varsigma(\varsigma^2-k^2)^2}X[J_0(\varsigma a)-J_0(\varsigma b)]^2 \tag{26}$$

Equation (26) preserves the original parameters of [11], which should be consulted for further details.

2.5.2 Model by Mosig et al.

According to reference [12], considering the general conditions shown in **figure 5** for the coaxial probe, 0 for a harmonic signal, the transverse fields on the coaxial linel ($z < 0$) are expressed by

$$E_{\rho}(\rho,z) = \boldsymbol{U_0}\left[f_0(\rho)e^{-\gamma_0 z} + \sum_{n=0}^{\infty} R_n f_n(\rho)e^{\gamma_n z}\right] \tag{27}$$

$$H_{\varphi}(\rho,z) = j\omega\varepsilon_0\varepsilon_c\boldsymbol{U_0}\left[\frac{f_o(\rho)}{\gamma_0}e^{-\gamma_0 z} - \sum_{n=0}^{\infty} R_n\frac{f_n(\rho)}{\gamma_n}e^{\gamma_n z}\right] \tag{28}$$

where the terms have the notation of the original article [12].

The coefficient $n = 0$ ccorresponds to the TEM wave and $n > 0$ corresponds to the higher order modes. For the TEM mode, one has

$$f_o(\rho) = N^0/\rho \tag{29}$$

For the modes TM_{0n}, $n > 0$, we have

$$fn(\rho) = Nn[J^1(\rho n\rho)Y^0(\rho na) - Y^1(\rho n\rho)J^0(\rho na)] \tag{30}$$

where $J_m(x)$ is the Bessel function of the first species and $Y_m(x)$ It is the Bessel function of second kind of order m. Details about generalization factor and eigenvalues of eigenvalues can be found in Mosig et al. [15]

The radial dependence of the transverse electric field of mode n is it is represented by the real function $f_n(\rho)$.

The complex coefficient R_n is the generalized reflection factor of the TM_{0n}, mode, defined by the ratio of the transverse electric field amplitudes reflected by the incident field thus in the plane $z = 0$. R_0 is the generalized reflection factor of the TEM mode.

The reflection factors R_n are unknowns of the problem and their values are determined by the procedure:

1. We must express the magnetic field on the right side ($z > 0$) in terms of the electric field in the opening plane;
2. Combine the magnetic field components over the boundary in the aperture plane ($z = 0$);
3. Evaluate numerically the integral expressions obtained for each mode in the structure;
4. Solve the matrix equation obtained with the mode matching techniques;
5. Determine the number of terms required for the desired accuracy;
6. Repeat the procedure for different values of ε_r; It is
7. Draw a graph $R_0(\varepsilon_r)$.

For circularly symmetrical field opening and distribution, in the absence of free loads, the field in the regionz > 0 is given by considering the line coaxial values

$$H_{\phi}(\rho,z) = \frac{j\varepsilon_m(\omega/c_0)^2}{2\pi\omega\mu_0}$$

$$\int_a^b\int_0^{2\pi} E_{\rho}(\rho')\frac{\exp\left(-j\frac{\omega}{c_0}\sqrt{\varepsilon_m}r\right)}{r}\rho' cos\psi \tag{31}$$

With;

$$\psi = (\phi - \phi') \tag{32}$$

$$r = \sqrt{(\rho^2 + \rho'^2 - {}^2\rho\rho' cos\psi + z^2)} \tag{33}$$

where (ρ', ϕ') are the transverse coordinates of the central point within the aperture and r is the distance from the point to the observer. The continuum $H_\phi(\rho, z = 0-) = H_\phi(\rho, z = 0+)$ results in an infinite set of equations for Rn ($n = 0,1,2, \dots$)

$$\sum_{n=0}^{\infty} T_n(\rho) R_n = 1 \tag{34}$$

Where;

$$T_n(\rho) = \frac{f_n(\rho)/\gamma_n + (\varepsilon_r/\varepsilon_c) I_n}{f_0(\rho)/\gamma_0 - (\varepsilon_r/\varepsilon_c) I_0} \tag{35}$$

$$T_n(\rho) = \frac{1}{2\pi}\int_a^b f_n(\rho)\rho' \int_0^{2\pi} \frac{\exp\left(-j\frac{\omega}{c_0}\sqrt{\varepsilon_m} r\right)}{r} cos\psi d\rho' d\psi \tag{36}$$

$$r = \sqrt{(\rho^2 + \rho'^2 - 2\rho\rho' cos\psi)}$$

In approaching the problem, only a finite number of modes are considered. The admissibility sought is determined by

$$\bar{Y} = \frac{1 - R_0}{1 + R_0} \tag{38}$$

The main disadvantage of this model is the need for intricate calculations, especially by using iterative methods for solving the inverse problem for a sufficient number of modes.

2.5.3 Model by Langhe et al

In the model by Langhe et al. [13], a multilayer MUT is assumed and high-order modes are taken into account. According to the authors, inconsistencies were found during the measurement of samples of different thicknesses with the Levine and Papas model [11]. The model derived by Langhe et al. [13] used the spectral domain technique, thus obtaining a closed-form expression for the admittance of an open-ended (flanged) coaxial line radiating into a stratified planar material terminated by a metal plate. This new expression can be considered as a correction for the Levine and Popes model [11]. The model considers the effects of dominant mode and higher-order modes. With this model measurements of low dielectric constant materials were performed along with an analysis of the perturbation of the influence of air bubbles (between the probe and the sample). Its admittance equation is given by

$$Y_0 = -\mathrm{j}\frac{\omega\epsilon_1}{c\sqrt{\epsilon_c}}\frac{1}{\ln\frac{b}{a}}\int_0^\infty d\lambda\, M(\lambda)\left[\frac{1}{\Gamma_1\lambda}(J_0(\lambda b) - J_0(\lambda a))^2\right]$$
$$-j\frac{\omega\epsilon_1}{c\sqrt{\epsilon_c}}\sum_{q=1}^{\infty}\frac{A_q}{A_0\,[1+K]}\int_0^\infty d\lambda$$
$$\cdot\frac{\varsigma_q\lambda^2}{\varsigma_q^2 - \lambda^2}\frac{M(\lambda)}{\Gamma_1\lambda}\left(J_0(\lambda b) - J_0(\lambda a)\right)$$
$$\left(bJ_0(\lambda b)R_1(\varsigma_q b) - aJ_0(\lambda a)R_1(\varsigma_q a)\right) \tag{39}$$

where the terms have the notation and meanings of the original article [13].

2.5.4 Pournapopoulous and Misra

In the formulation of the quasi-static model, it is considered that only the fields in the TEM mode are present over the coaxial opening. However, according to Pournapopoulous and Misra [15], these fields can be determined precisely by solving the equation for the radial component of the electric field $E\rho(\rho', ^0)$ over the aperture:

$$\frac{1}{\rho} + j\pi\omega\varepsilon_r.\varepsilon_0 \int_a^b E_\rho(\rho',0)K_c(\rho,\rho')\rho' d\rho' = j\omega\varepsilon_r.\varepsilon_0(1 - j\tan\delta) \int_a^b E_\rho(\rho',0)\rho' d\rho' \int_0^\pi \cos(\phi)\frac{\exp(-jkr)}{r}d\phi' \quad (40)$$

$$E_z(\rho,z) = \frac{1}{\pi}\int_a^b E_\rho(\rho',0)\rho' \int_0^\pi \cos(\phi')\frac{\exp(-jkR')}{R'} x \left[\frac{1}{\rho} - \left(jk + \frac{1}{R'}\right)\frac{\rho - \rho'\cos(\phi')}{R'}\right] d\phi' d\rho \quad (41)$$

$$Y_L = \frac{2}{\int_a^b E_\rho(\rho',0)d\rho'} - \frac{2\pi}{\left[\sqrt{\frac{\mu_0}{\varepsilon_0\varepsilon_l}}\, ln\left(\frac{b}{a}\right)\right]} \quad (42)$$

Equation 42 is solved numerically (method of moments) for the aperture field $E\rho(\rho', ^0)$ of a coaxial line opening in a material medium [15].

From several tests and analyzes, Misra [15] concluded that the radial and axial field components decay very quickly with increasing horizontal distance from the central conductor (radial fields $E\rho$) and as the distance from the aperture plane $z = 0$ (axial fields Ez) increases. Thus, the variational expression for the opening admittance (proposed by Marcuvitz [9]) may be a good approximation, even if the presence of high order modes is ignored.

2.6 Rational function model

The Rational Function Model (RFM) [16] is accurate and has wide operating frequency range. It is an approximation of the solution of the Method of Moments of the complete wave.

The RFM model, compared to previous models, offers better accuracy and allows uncertainties in dielectric measurements to be quantified. The normalized aperture admittance equation for the coaxial probe, on a 50 Ω, coaxial cable whose line is filled with Teflon, is given by

$$Y = \frac{\sum_{n=1}^{4}\sum_{p=1}^{8}\hat{\alpha}_{np}(\sqrt{\varepsilon_r})^p(sa)^n}{1 + \sum_{m=1}^{4}\sum_{q=1}^{8}\hat{\beta}_{mp}(\sqrt{\varepsilon_r})^q(sa)^n} \quad (43)$$

where Y is the aperture admittance, εr it is the permittivity of the medium, s is the complex frequency, a is the radius of the inner conductor and $\hat{\alpha}_{np}$ and $\hat{\beta}_{mp}$ are coefficients of the model [16].

The admittance Y, as in the other models, refers to that normalized in relation to the coaxial line of 50 Ω.

The model is valid for permissivities in the ranges $1 \leq \varepsilon' \leq 80$, $0 \leq \varepsilon'' \leq 80$, over a normalized frequency range (k_0a) from 0.01 to 0.19 (1 to 20 GHz). Their coefficients and equations for obtaining them are presented in [16].

2.7 Bilinear transformation model

In the capacitive model, the complex permittivity is extracted from the reflection coefficient without considering the effects of radiation.

Bao et al. [17] demonstrated that the complex permittivity of a material under investigation can be determined from the reflection coefficient ("Raw GAMMA"). From **equation** 44 it is possible to determine the complex permittivity. However, Γ_{bruto} the real reflection coefficient ("GAMMA real"), measured at from the network analyzer. Therefore, in addition to the coaxial probe/material interface information, several error effects of the coaxial line, connectors and encapsulation are included in the value of Γ_{bruto}. These are systematic errors and, to eliminate them, the authors used a procedure of specific calibration (different from the standard) which is based on the assumption that the relationship between the reflection coefficient and the permittivity is bilinear.

This relationship can be represented mathematically by a two-port linear network as in **figure** 6

Fig. 6 – Ratio between Γ measured and ε afrom a 2-port linear network.

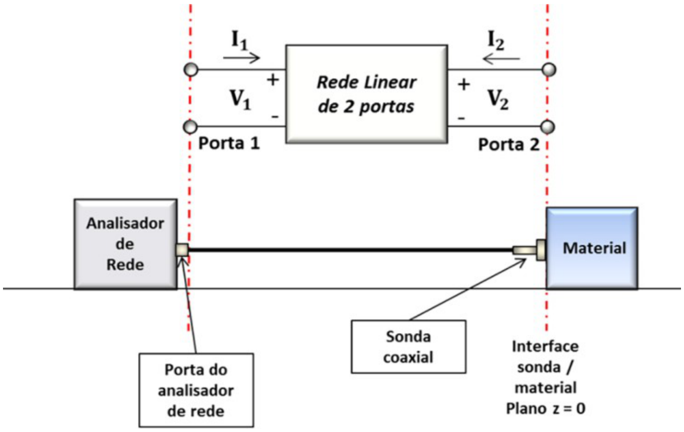

From this assumption, the use of three measurement patterns and some mathematical manipulations of the scattering matrix, the authors arrived at the equation

$$\varepsilon_r = \frac{A_1 \Gamma_{bruto} - A_2}{A_3 - \Gamma_{bruto}} \tag{44}$$

where A_1, A_2 and A_3 are three complex frequency-dependent constants related to the elements of the scattering matrix, the characteristic impedance Z_0 and the concentrated circuit elements (C_0 and C_f).

$$A_1 = \frac{1 - S_{22}}{j\omega Z_o C_0(1 + S_{22})} + \frac{C_f}{C_0} \tag{45}$$

$$A_2 = \frac{S_{11} - S_{11}S_{22} + S_{12}S_{21}}{j\omega Z_o C_0(1 + S_{22})} + \frac{C_f(S_{11} + S_{11}S_{22} - S_{12}S_{21})}{C_0(1 + S_{22})} \tag{46}$$

$$A_3 = \frac{S_{11} + S_{11}S_{22} - S_{12}S_{21}}{1 + S_{22}} \tag{47}$$

H. Blackham and Polllard model

In Misra's quasi-static model [9], one obtains the stationary expression by equating the tangential magnetic field expressions at $z = 0$. In [12], Misra used the simplifying assumption $E_r(r, 0) = E_0/r$ to obtain the stationary expression for the normalized aperture admittance, which is represented by

$$\bar{Y}_L = \mathrm{j}\frac{k^2}{\pi k_c \ln(b/a)} \int_a^b \int_a^b \int_0^\pi \cos\phi' \frac{\exp(-jkR)}{r}\, d\phi' d\rho' d\rho \tag{48}$$

Blackham and Pollard [18] transformed **equation** 48 in a Taylor series expansion (truncated in 28 terms). This yielded an expression where the integrals are independent of the characteristics of the medium. Since integrals are calculated for a given probe geometry, the resulting polynomial expression allowed rapid computation of the normalized aperture admittance:

$$Y_L = \frac{jk_m^2}{\pi k_c ln\left(\frac{b}{a}\right)}\left\{j\left[I_1 - \frac{k_m^2}{2}I_3 + \frac{k_m^4}{24}I_5 - \frac{k_m^6}{720}I_7 + \cdots\right] + \left[I_2 k - \frac{k_m^3}{6}I_4 + \frac{k_m^5}{120}I_6 - \cdots\right]\right\} \tag{49}$$

$$I_n = \int_a^b \int_a^b \int_0^\pi R^{n-2}\cos\phi\, d\phi' d\rho' d\rho$$

Where; (50)

VOL.39 Nº4 2022
https://doi.org/1022135\IMECTA.9896.en

The authors found, as expected, that the admittance calculated using (**equação** 49) deviates from the actual admittance because the high-order modes of the electric field in the aperture are not included in the model derivation.

In this way, they modified the constants I_n using values based on measurements up to 20 GHz of various materials with permissiveness values between the permittivity of air and water. Instead of optimizing each parameter individually, the parameters were grouped using the expression

$$I_n = \int_a^b \int_a^b \int_0^\pi R^{n-2} \cos\phi \, d\phi\,' d\rho' d\rho \tag{51}$$

In this way, the optimization parameters α, β and χ were adjusted until the admittance calculated through **equation** 49 provide the best marriage with royal admittance.

Table 1 presents the synthesis of the coaxial tip admittance models addressed in this work.

Tab. 1 - Summary of coaxial probe admittance models

Model	Main Characteristics
Capacitive	The discontinuity of the probe aperture is modeled as two capacitors in parallel Co e Cf [2]
Radiação	A radiation conductance G is added in parallel to the equivalent circuit of the Capacitive model [4][5]
Complete wave	Equations for the regions $z < 0$, $z = 0$ and $z > 0$ of the probe/material system are modeled by means of a variational method. [15]
Quasi-static	Serial expansion for truncation in 3 terms and quasi-static approximation of the Marcuvitz model [11] for the probe aperture. [9]
Marcuvitz Expanded	Serial expansion and truncation in 7 terms for the Marcuvitz model [8] for the probe aperture. [10]
Bilinear transformation	It uses the concept of a two-port linear network (with S parameters) to model the linear relationship between permittivity and reflection coefficient. [17]
Rational Function	Equations for the regions $z < 0$, $z = 0$ and $z > 0$ of the probe/material system are obtained by the method of moments and the solution to such equations is approximated by a rational function. [16]
Enhanced quasi-static for higher order modes	The Misra solution [9] for the opening admittance is improved by means of actual values of admittance, in order to account for high order modes generated by the discontinuity of the opening. [18]

3. Permittivity Extraction Schemes

In the process of extracting complex permittivity from a measured datum, when the solution of the inverse problem does not have an explicit equation, some recursive optimization technique is used. Among the most common, we can mention: Nelder and Mead, Newton, Simplex, Genetic Algorithm (GA) and Particle Swarm Optimization (PSO) .

According to Peres [19], they help in the selection of the extraction scheme:

a. Modularity
b. Interconnectability
c. Robustness
d. Speed
e. Accuracy
f. Computational cost

These parameters are related to the characteristics of each model. In the present work, three extraction schemes based on the Simplex Point Matching, Gradient Point Matching and Particle Swarm Optimization (PSO) algorithms are presented, which are detailed in [19].

3.1 Scheme 1 - Simplex Point Matching

A suitable scheme for extracting a permittivity value from an admittance equation is the Simplex Point Matching algorithm [19]. In this scheme it is necessary to create a permissiveness table whose elements are the input data domain for the search defined by the analysis window (maximum and minimum permissiveness considered) and by the resolution (distance between elements).

Through this permissiveness table, the admittance model is created. From the table of admittances, the element which approximates the best measured value. Once the association between admittance elements and permittivity elements is maintained, it is possible to recover the permittivity and the estimation ends.

3.2 Scheme 2 - Gradient Point Matching

In this method a permissiveness table is not calculated as in the previous method. The same analysis windows are defined and then decisions are made about how a movement in the permittivity plane affects the admittance plane, so as to get closer to the measured value. In this way, estimation is used.

There is an initial state, where ϵ_0 is the starting point in the permissiveness domain to start the search. The separation vector is considered as a proximity indicator (proximity to the measured admittance in the admittance domain). O vetor de separação ΔYo é considerado como um indicador de proximidade (proximidade à admitância medida no domínio da admitância).

Since a displacement in the permittivity plane corresponds to an unknown displacement in the admittance plane, a tester vector (seeker) is used to analyze all directions (usually 8 are considered), with normalized pitch (the magnitude of the movement is a fixed value) , which is the response in the admittance plane used as an indication of how good the proximity indicator ΔY is.

The starting point for each research step is called the Actual Point denoted as ϵ_A e Y_A and on each plane, respectively. The end-point of each research step is called the Future Point and is denoted as ϵ_F and Y_F on each plane, respectively.

3.3 Scheme 3 - Particle Swarm Optimization (PSO)

It is a metaheuristic computational method that optimizes a problem by iteratively trying to improve a candidate solution with respect to a given quality measure.

PSO optimizes a problem by having a population of candidate solutions (particles) and by moving these particles around the search space according to simple mathematical formulas about the position and velocity of the particle.

The motion of each particle is influenced by its best-known local position and is also oriented to the best-known positions in the search space. These in turn are updated as better positions are found for other particles. The particle swarm is expected to be moved to the best solutions.

4. Comparison Between Models

In defining an admission model, the application of interest must be taken into account. Each model has properties that relate to the parameters of the measurement system (speed, accuracy, maximum frequency, need for calibration, use of reference materials, etc.). It must also be compatible with the physical dimensions of the probe used. The most important properties are described in the following items and listed in **table** 1, which presents the comparison of the models treated in this article.

4.1 Closed expression for inverse solution

Coaxial probe models establish a bidirectional mapping between the admittance at the probe aperture and the complex permittivity of the test material. The mathematical expressions of each model vary from smallest to largest complexity. There are models whose variable of interest (ε*) can be isolated algebraically and therefore have a closed expression for the inverse solution. This is the case of the models of items [2], [4], [17].

For the other models, direct expressions do not allow ε* to be isolated, requiring the use of numerical techniques to solve the inverse problem.

4.2 Computational cost

Os modelos que não levam em consideração os modos de ordem elevadas na abertura da sonda e cuja solução para o problema inverso é uma expressão fechada, apresentam baixo custo computacional. É o caso dos modelos da capacidade, da radiação e da transformação bilinear. Os demais modelos apresentam maior complexidade matemática para a solução direta ou a solução inversa requer a utilização de alguma técnica de otimização.

Models that do not take into account the high order modes at the opening of the probe and whose solution to the inverse problem is a closed expression, have low computational cost. This is the case of the models of capacitance, radiation and bilinear transformation. The other models present greater mathematical complexity for the direct solution or the inverse solution requires the use of some optimization technique.

The criteria adopted to evaluate the computational cost is based on the equation of the models as follows:

1. Equations with first and second order polynomials: low computational consumption.

2. Equations with divisions, roots, polynomials of order 3 or greater: average computational consumption.

3. Integral equations, derivatives, logarithms: high computational consumption.

4.3 Upper Frequency Limit

In most cases, models that do not account for the presence of higher-order modes in the aperture are not applicable at high frequencies. As noted in [5], the capacitive and radiation models are restricted respectively to the limits of 2 and 6 GHz.

In quasi-static and expanded Marcuvitz models, which use serial expansions of Marcuvitz equations, the upper frequency limit is proportional to the number of terms used. The Blackham & Polard model, being a form of the Marcuvitz equation truncated in 28 terms, has a frequency limit of 20 GHz.

In the bilinear Transformation model, which is based on the Capacitive model, the effects of radiation are reduced from calibration, which is in the computation of the direct solution coefficients.

In an improved version of the bilinear transformation model [22], although the effects of radiation are not included in the equivalent circuit, it has been shown analytically that errors due to radiation can be reduced with the implementation of an additional calibration procedure, especially when the dielectric properties of the materials under test are close to the calibration standards.

The full wave models and the rational function model, in principle, are not limited in frequency, since the higher modes are considered in the formulation. Its authors, however, made measurements up to the frequency of 20 GHz only.

4.4 Use of Reference Materials

Most coaxial probe admittance models use reference materials to determine the direct solution expression parameters. Among those analyzed are the capacitive, radiation, rational function, and bilinear transformation models by Blackham & Polard.

Typical reference materials are water, air and alcohols whose frequency permittivity responses can be described by Debye relaxation models.

4.5 Need for Network Analyzer Calibration

In measurements with the coaxial probe using analyzers of networks, the error model of an analyzer port is used. This model describes the systematic errors included in the measures.

On the bench, the raw reflection coefficient of the probe (uncorrected) is obtained from the network analyzer. In the usual procedure of most models, the network analyzer is calibrated in a first step, to compensate for systematic errors in the reflection coefficient measures, and the permissiveness of the MUT is calculated with the probe model. The bilinear transformation model uses a particular calibration procedure, in which its bilinear relationship is also used to quantify systematic errors from the measurements of the reference materials. Thus, in this model, the effect of systematic errors are embedded in the solution of the direct problem.

4.6 Restriction on probe diameter

Conforme [20], os modelos baseados em circuito equivalente concentrado (modelo capacitivo, da radiação, da transformação bilinear) e o modelo quase estático, são aplicáveis somente a sondas com diâmetro entre 3 e 6 mm.

O modelo de Blackham e Pollard [18] pode ser aplicado em qualquer situação, pois, segundo os autores, não depende da frequência e das características do meio, mas somente da geometria da sonda. Estendendo tal consideração para o modelo de Marcuvitz expandido, pode-se concluir que a expansão em até sete termos é válida somente para a sonda coaxial do respectivo estudo, que têm diâmetro em entre 3 – 6 mm.

Os modelos de onda completa e o da função racional não estão limitados em relação à geometria da sonda.

4.7 Model Accuracy

The accuracy of the model is related to how close the results obtained from the model are to the actual results of the material. To evaluate the accuracy in this work, the permissiveness curves (real part and imaginary part) obtained by each model were compared with permittivity data available in the literature. For this purpose, we used the relative error percentage given by

$$E_{RP} = \left(\frac{\varepsilon_{estimado} - \varepsilon_{real}}{\varepsilon_{real}}\right)100\% \tag{52}$$

where $\varepsilon_{estimado}$ is the complex permittivity (actual part or imaginary part) measured by the user, ε_{real} is the complex permittivity (real part or imaginary part) of the material.

For comparison purposes, the following scale was used:

- $< 5\%$: High Accuracy
- $5\% < < 10\%$: Average accuracy
- 10%: Low Accuracy

The accuracy data in **table** 2 were determined from an approximate graphical analysis of the results of each model at the frequency of 6 GHz exclusively, except for the quasi-static model, whose analysis was performed at 3 GHz.

Tab. 2 - Detailed comparison between admittance models

MODEL	Closed expression for inverse solution	Computational Consumption	Upper Frequency Limit	Use of Reference Materials	Systematic errors embedded in the model	Restriction on probe diameter	Accuracy / E_{RP}
Capacitive model	✓	LOW	2 GHz	YES	✕	RESTRICTED	LOW / 12,15%
Tilt radiation model (i)	✓	LOW	6 GHz	YES	✕	RESTRICTED	HIGH / 4,88%
Tilt radiation model (ii)	✓	LOW	6 GHz	YES	✕	RESTRICTED	No information
Tilt radiation model (ii)	✓	LOW	2,5 GHz	YES	✕	RESTRICTED	HIGH / 0,97%
Quasi-static model	✓	MEDIUM	10 GHz	NO	✕	RESTRICTED	LOW / 16,3%
Expanded Marcuvitz model	✕	MEDIUM	18 GHz	NO	✕	RESTRICTED	AVERAGE / 6,25%
Full Wave Models (i)	✕	HIGH	No information	NO	✕	UNLIMITED	No information
Full Wave Models (ii)	✕	HIGH	10 GHz	NO	✕	UNLIMITED	HIGH / 0,5 %
Full Wave Models (iii)	✕	HIGH	20 GHz	NO	✕	UNLIMITED	LOW / 21,38 %
Full Wave Models (vi)	✕	HIGH	10 GHz - 20 GHz	NO	✕	UNLIMITED	HIGH / 3,92%
Rational Function Models	✕	HIGH	20 GHz	YES	✕	UNLIMITED	HIGH / 3,3%
Bilinear transformation model	✓	LOW	26 GHz	YES	✓	UNLIMITED	HIGH / 4,36%
Blackham & Pollard Model	✕	HIGH	20 GHz	YES	✕	UNLIMITED	HIGH / 2,05%

5. Conclusions

The present article presents important concepts about the use of dielectric characterization models of materials with the coaxial test tip method. They were approached from models that are based on an approximation through equivalent circuits, to models based on rigorous electromagnetic analysis of the problem.

From the research carried out, **table** 2 was generated, which presents a comparative analysis of the various models evaluated. Depending on the desired application, a quick consultation of the Table may provide indications of which methods are suitable, or which are not, for the intended measures.

The most appropriate models are suggested in relation to important measurement parameters: considering the frequency range - they are the full wave and rational function models; considering computational consumption - the radiation and bilinear transformation models are quite appropriate, considering reference materials - the rational function and Blackham & Pollard and bilinear transformation models are adequate. Finally, considering accuracy, the rational function and Blackham & Pollard models are remarkable, as high order modes are considered and compensated for.

To the final reader, I indicate the bilinear transformation model for commercial use and the rational function model for use in scientific research.

This article provides an overview and guidance for those wishing to develop permittivity measurement systems from the coaxial probe.

Subtle and relevant information and details scattered in numerous references on the subject have been synthesized in this article.

Thanks

This study was funded by the Coordination for the Improvement of Higher Education Personnel – Brazil (CAPES) – Financing Code 001. The authors are also grateful to the Microwave Laboratory team, which provided all the necessary assistance in the assembly of measurement setups and in the search for solutions to practical and theoretical problems.

References

[1] Chen, L.F. Ong, C.K. Neo, C.P. Varadan, V.V. and Varadan, V.K. (2004). “Microwave Electronics Measurement and Materials Characterization”, John Wiley & Sons Ltd, England.

[2] T. W. Athey, M. A. Stuchly, S. S. Stuchly. “Measurement of radio frequency permittivity of biological tissues with an open-ended coaxial line: part I” IEEE Transactions on Microwave Theory and Techniques, vol. 30, no. 1, pp. 82-86, Janeiro, 1982.

[3] T. W. Athey, M. A. Stuchly, G. G. Samaras, G. E. Taylor. “Measurement of radio frequency permittivity of biological tissues with an open-ended coaxial line: part II – Experimental results” IEEE Transactions on Microwave Theory and Techniques, vol. 30, no. 1, pp. 87-92, Janeiro, 1982.

[4] M. A. Stuchly, M. M. Brady, S. S. Stuchly, G. Gadja. “Equivalent circuit of an open-ended coaxial line in a lossy dielectric”. IEEE Transactions Instrumentation and Measurement, vol. 31, no. 2, pp. 116-119, Junho, 1982.

[5] Liao et al, “An Accurate Equivalent Circuit Method of Open Ended Coaxial Probe for Measuring the Permittivity of Materials” Selected Papers from the 2011 International Conference on Electric and Electronics (EEIC 2011) in Nanchang, vol. 3, pp. 779-784, Junho 2011.

[6] G. B. Gajda, S. S. Stuchly. “An Equivalent Circuit of an Open-Ended Coaxial Line” IEEE Transactions on Microwave Theory and Techniques, vol. 32, no. 4, pp. 506-508, Dezembro, 1983.

[7] N. K. F. Staebell, D. Misra. “An experimental technique for in vivo permittivity measurement of materials at microwave frequencies” IEEE Transactions on Microwave Theory and Techniques, vol. 38, no. 3, pp. 337-339, Março, 1990.

[8] Marcuvitz, Ed. New York: McGraw-Hill, 1951, pp. 213-216.

[9] D. Misra. “A quasi-static analysis of open-ended coaxial lines” IEEE Transactions on Microwave Theory and Techniques, vol. MT=35, pp. 925- 928, Outubro, 1987.

[10] D. Misra, M. Chabbra, B.R. Epstein, M. Mirotznik, K. R. Foster. “Noninvasive electrical characterization of materials at microwave frequencies using an open-ended coaxial line: Test of an improved calibration technique”. IEEE Transactions Instrumentation and Measurement, vol. 38, pp. 8-14, Janeiro, 1990.

[11] H Levine and C. H. Papas. “Theory of the circular diffraction antenna,”J. Appl. Phys., vol. 22,- pp. 29-43: 1951.

[12] J. R. Mosig, J. C E. Besson, M. Gex-Fabry, F. E. Gardiol. “Reflection of an open-ended coamal line and application to nondestructive measurement of materials” IEEE Transactions Instrumentation and Measurement, vol. IM-30, no. 1, pp. 46–51. Março, 1981.

[13] P. De Langhe, L. Martens e D. De Zutter, “Measurement of Low Permittivity Materials Based on a Spectral-Domain Analysis for the Open-ended Coaxial Probe” IEEE Trans. Instrum. Meas., vol. 42, no. 5, pp. 879-886, Outubro, 1993.

[14] C. L. Li and K. M. Chen, “Determination of electromagnetic properties of materials using flanged open-ended coaxial probe-Full wave analysis” IEEE Trans. Instrum. Meas., vol. 44, pp. 19-27, Fevereiro, 1995.

[15] D. Misra, “On the measurement of the complex permittivity of materials by an open-ended coaxial probe.” IEEE Microwave Guided Wave Lett., vol. 5, pp. 161-163, Maio, 1995.

[16] Anderson J. M., C. L Sibbald, S. S. Stuchly, “Dielectric Measurements Using a Rational Function Model”. IEEE Transactions on Microwave Theory and Techniques, vol. 42, no. 2, pp. 199-204, Fevereiro, 1994.

[17] Z. J. Bao, C. C. Davis, L. M. Swicrod, “Microwave Dieletric Measurements of Erythrocyte Suspensions” Biophysical Journal, vol. 66, pp. 2173-2180, Junho, 1994.